Signal Processing 132 (2017) 210–220

Contents lists available at ScienceDirect

Signal Processing

journal homepage: www.elsevier.com/locate/sigpro

Review of multi-offset GPR applications: Data acquisition, processing and analysis

Emanuele Forte *, Michele Pipan

Department of Mathematics and Geosciences, University of Trieste, Via Weiss, 1-34128 Trieste, Italy

ARTICLE INFO

Article history:
Received 29 January 2016
Received in revised form
8 April 2016
Accepted 21 April 2016
Available online 27 April 2016

Keywords:
Multi-fold
Multi-offset
GPR
AVO
Stacking
EM velocity

ABSTRACT

GPR and reflection seismics share common physical and methodological bases but are sensitive to different subsurface physical properties. The peculiarities of the electromagnetic case impact data acquisition, processing and interpretation. We review multi-offset techniques in GPR applications focusing on similarities and differences through examples taken from different subsurface and target conditions.

GPR multi-offset data acquisition methods basically involve common-offset and common midpoint geometries: accuracy and work load are the main factors that drive the choice, together with effectiveness of the solution for the objectives of the study.

Multi-fold data processing algorithms can bring remarkable signal-to-noise ratio enhancement and offer the opportunity to extract additional information from field data. Velocity field and related dielectric constants distribution, attenuation and related conductivity variations, changes in the GPR response with offset are some of the examples. Coherent noise suppression and velocity analysis are key features in GPR multi-fold processing sequences and we review the relevant methods with examples of application in addition to technical aspects.

Multi-channel acquisitions, full wave-form inversion, pre-stack depth migration, azimuthal and polarimetric analysis, are among the many topics in current and future research that are briefly reviewed to provide some highlights of the forthcoming developments in GPR methods.

1. Introduction

In many archeological, engineering, environmental, and geological applications, ground-penetration radar (GPR) is nowadays an important geophysical tool to investigate the shallow subsurface (e.g., [30,53]).

Typical GPR surveys are collected in common offset (CO) or single-fold (SF) mode. CO acquisition deploys one transmitting and one receiving antenna that move together along the surface keeping a constant offset. Such configuration is also reposted as bistatic because it uses two antennas with separated transmitting and receiving functions. When a single antenna acts alternately as transmitting or receiving one (monostatic configuration) we have zero-offset conditions. In a CO survey a fixed geometry is usually applied, using not only a constant separation but also a fixed orientation between the antennas.

The first applications of multi-fold (MF) methods to GPR investigation date back to the early 1970s [44] but only in the 1990s the advances in GPR technology, namely the advent of low cost, portable digital units as well as the extension of GPR applications to increasingly complex exploration targets enlarged the interest to these methods. The basic meaning of MF is that each subsurface point is imaged by multiple ray paths (or, better, wavefronts), while in the SF the information about each subsurface point comes from a single ray (wavefront). MF techniques are the basis of reflection seismic data acquisition and processing since the 1960s of last century and contributed to the exponential growth of such method soon after the digital recording revolution [72,88]. Seismic processing techniques can be applied to GPR data due to similarities between seismic and high-frequency electromagnetic wave propagation. Several studies explored in detail the theoretical correlations between the kinematics of the two wave field methods [21,23,80]. The main differences regard the perturbing field characteristics and in particular the vectorial character of electromagnetic waves compared to the scalar nature of acoustic ones. Obviously there are important differences in physical parameters such as frequency, velocity, impedance and, clearly, some scaling factors.

Before the 1990s, signal processing applied to SF GPR data was minimal but with the advent of digitally recording radar systems new possibilities opened and several algorithms previously applied only to reflection seismic data were adapted to GPR processing [37]. Since that time more complex processing flows and

* Corresponding author.

http://dx.doi.org/10.1016/j.sigpro.2016.04.011
0165-1684/

dedicated analyses have been proposed and tested extending the applicability of the GPR and overcoming some limitations on the complexity of structures that could be reliably investigated with such geophysical tool.

In this paper we focus on MF technique by analyzing its peculiarities in GPR application in terms of data acquisition, processing and analysis, to provide a comprehensive and critical review. Future implementations made possible by recent hardware upgrades are further considered and evaluated.

2. Data acquisition

In reflection seismics the MF expression is usually considered a synonymous of "multi-channel" because a standard MF survey encompasses several (from tens to several thousands) receiving sensors (geophones or hydrophones) to record the kinematic and dynamic information (i.e. arrival times and amplitudes) of a wave field produced by a seismic source. The most common commercial GPR systems are, on the other hand, "single-channel-devices", since they have just one receiving antenna to record the EM field produced by the transmitting antenna. Therefore MF data acquisition geometries should be tailored to be applicable to "single-channel" instruments. Disregarding the variations of the antenna azimuth (i.e. keeping the azimuth constant during the acquisition) there are three convenient acquisition geometries that can be used to collect MF data sets (Fig. 1). The easier way is to symmetrically increase the offset of the antennas while keeping fixed the midpoint between them (Fig. 1a). This acquisition geometry is usually referred as Common Midpoint Gather (CMP) as in reflection seismics. In the following, it will be referred as case (A). An alternative way is to move just one antenna away from the other usually recording the traces at increments multiple of a certain fixed step (B). This acquisition geometry is conceptually identical to the one used for marine seismic data acquisition with a single source and several receivers that are reproduced in the GPR case by the progressive displacement of one of the antennas. Therefore, a single Common Source (or shot) Gather (CSG) or Common Receiver Gather (CRG) is different from a CMP gather because the wavefronts illuminate different subsurface positions (Fig. 1b). Anyway, if we collect a series of CSG or CRG laterally shifted by a constant distance, it is still possible to rearrange (sort) the data into series of CMP gathers (Fig. 1b). It is interesting to highlight that in seismic surveys the data are usually recorded as CSG (by using multi-channel systems) and are then rearranged as CMP before data processing. There is another way to obtain MF data by using just one transmitting and one receiving antennas, by acquiring several CO profiles along the same path each with a different offset (Fig. 1c) (C). Also in such case it is possible to reconstruct the CMPs taking into account the locations of both antennas at each acquisition position.

As shown in Fig. 1, the maximum fold can vary as a function of the adopted geometry and survey parameters like the source (in seismic "shot") interval. In fact, while in (A) the maximum fold is fixed by the number of measurements, which in turn depends on the offset increments, in the other two cases the fold is not constant along the profile and has a more complex dependency. For the case (B) the maximum fold F_{max} is given by the relation:

$$F_{max} = N\Delta_{off}/2\Delta_{SH} \tag{1}$$

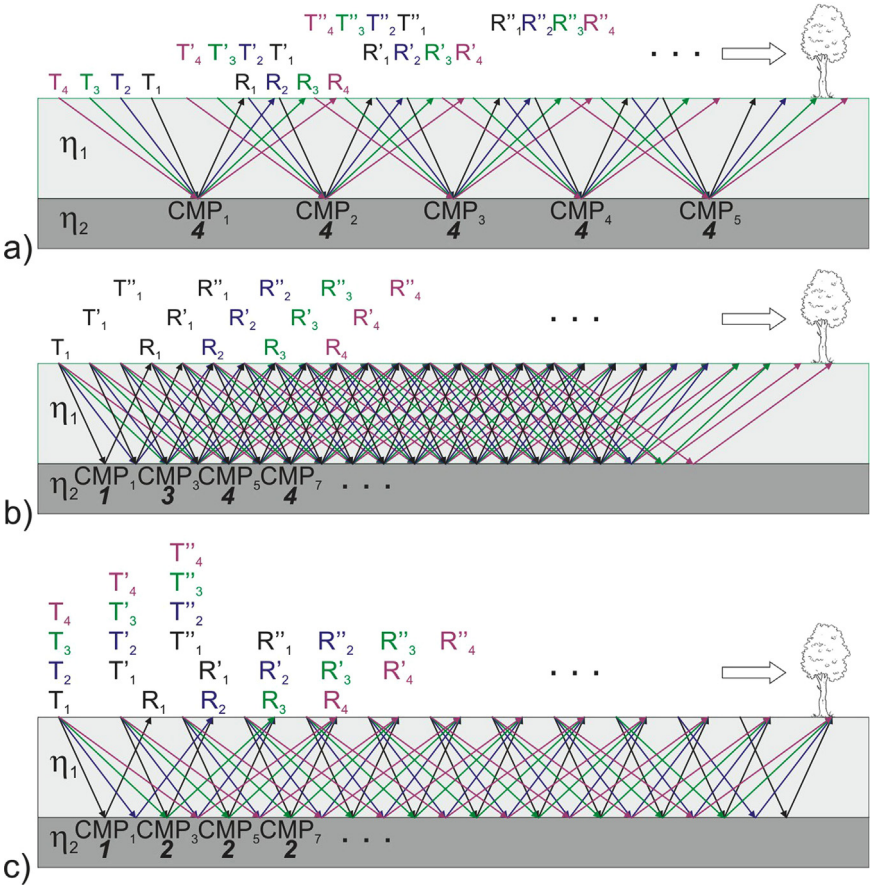

Fig. 1. Acquisition schemes for MF data acquisition with single channel GPR devices: (a) series of CMP gather; (b) series of CSG; and (c) series of CO profiles. T refers to the transmitting antenna positions, while R to the receiving ones. Labels in bold indicate the CMP fold.

where N is the number of receiver positions, Δ_{off} is the offset increment (receiver spacing) and Δ_{SH} is the source spacing.

If such parameters are randomly chosen then the fold can be very low (at the limit just one) even if several CSG or CRG made by a lot of traces are collected.

In the case (C), the maximum achievable fold is equal to the number of collected profiles; such result is obtained when:

$$\Delta_{SH}=\Delta_{off}/2 \tag{2}$$

or just by keeping fixed the location of the first midpoint of each offset. Fig. 1 shows that there is a decrease of the fold at both ends of the profile but in the (A) case. It is therefore advisable to extend the profiles in order to achieve a constant maximum fold in the zone of interest, thus preventing possible lateral variations of the signal-to-noise ratio (S/N).

From the logistical point of view it is quite obvious that the most efficient geometry is (C) followed by (B) where just one antenna is moved, and finally (A), which requires the maximum acquisition time. On the other hand, in terms of accuracy the best strategy is (A) while the less precise is (C) because is not so straightforward to follow the same path several times. Bradford et al. [16,17] applied an interesting hybrid acquisition geometry, using a multi-channel GPR connected with one transmitting and three receiving antennas. Data were acquired in a total of five passes of the set of four antennas along the same path, with a different offset range on each. This way a maximum fold of 15 was obtained in a relatively easy and rapid way.

All the above described procedures suffer from some constraints and limitations that depend on the physics of the EM wave propagation and on the instrumentation. Since the antenna dimensions have an inverse correlation with their central frequency due to physical constraints (e.g. [29]) and can be larger than 1 m for frequencies lower than about 100 MHz, the minimum offset for a bistatic antenna pair cannot be too small. Moreover, several commercial systems use shielded antennas, which are bigger than the corresponding unshielded ones. In addition to these logistical constraints there are some physical limitations that cannot be overcome. GPR systems are designed to propagate EM waves, which can be considered planar far away from the source. The immediate vicinity (less than about one wavelength) of an antenna is usually referred as “near field”, and is characterized by a strong electromagnetic field that theoretically prevents true wave propagation, as this energy is not yet coupled with the ground [27]. Therefore, in the GPR experiments the offset should be set large enough to assure far field conditions, even if there are some recent works [35,74] where the near field is used to extract information from the subsurface. On the other hand, the offset cannot be too large especially where high conductive subsurface materials are present. In fact, the larger is the offset, the longer is the ray path of the reflections and the attenuation of EM waves may reduce the amplitude of the wave field below the sensitivity threshold of the receiving antenna. Moreover, when the offset is large compared to the depth of the targets, the small spread approximation (SSA) cannot be considered valid anymore and the reflection traveltimes cannot be approximated by simple hyperbolas [88]. It is therefore advisable to limit the maximum offset to exploit analysis and processing algorithms based on SSA, like velocity analysis and stacking.

In addition to the MF data acquisition with variable offset but fixed azimuth, multi-azimuth and polarimetric surveys exploit the vectorial radiation characteristics of GPR antennas, which show marked angle-dependent amplitude and polarization variations [82,83].

A brief review of such applications will be provided in the following section; here we highlight the possible acquisition geometries and their implementation with a bistatic single channel system, postponing the description of multi-channel and multi-array devices in the discussion.

Fig. 2 gives a sketch of all the possible geometries between two antennas, considering that: they can be co- or cross-polarized, they can have the electric field vector oscillating along (TM mode) or perpendicular (TE mode) to the survey direction, and they can be oriented with their end points toward each other (End fire configuration) or with the broad sides toward each other (Broadside configuration).

To summarize we can remark that even if usual GPR surveys are performed in TE broadside configuration, which is sometimes also reported as perpendicular or transverse polarization (e.g. [53]), there are many other possible options. With just one transmitting and one receiving antennas we showed that there are several methods to obtain MF data, which are a special case of the more general category of the “multi-offset constant azimuth” surveys. In fact, if we vary the azimuth of one or both antennas during the acquisition we can record “single or multi-offset multicomponent” data sets, while changing the orientation of one or both antennas with respect to a target we acquire “single or multi-offset polarimetric” data sets. The two latter options were analyzed from the theoretical point of view and by forward modeling [52,81–83,85,75] but they are still not fully exploited for real extensive acquisitions.

3. Data processing and analysis

Data processing encompasses all the steps required to extract from any dataset all the useful information. It is conceptually different from “data analysis” because it refers to any algorithm that modifies the original data while the analysis encompasses temporary operations preliminary to processing steps or useful to achieve improved data component visualization and discrimination. Several of the algorithms that can be conveniently applied to GPR data were originally developed for reflection seismics or, in some cases, for image processing (e.g. [26]). It would be impossible to summarize here all the methods proposed to process different types of GPR data, but it is important to notice that they cannot be unified in a single and “standard” processing flow. Objectives of the survey as well as characteristics of site and data should drive the design of the processing sequence and the choice of the optimum parameters. In very lucky situations, where the subsurface is extremely uniform and simple and/or targets and background have a great EM contrast, the data could be interpreted without any preliminary processing, but these are indeed very uncommon cases. At least one procedure is almost always mandatory, namely the amplitude compensation (or gain). This is due to the high intrinsic attenuation of most materials [30] which makes it impossible to detect clear reflections even when they are related to relatively shallow interfaces.

3.1. Review of the velocity analysis techniques

In lossy media, the velocity of a transverse EM wave v_m within a material having electric conductivity σ, dielectric permittivity ε and magnetic permeability μ is given by (e.g. [4])

$$v_m = \left[\frac{\mu\epsilon}{2}\left(\sqrt{1+\tan^2\,\delta}+1\right)\right]^{-1/2} \tag{3}$$

where $\tan\,\delta$ is the loss tangent equal to:

$$\tan\,\delta = \frac{\sigma}{\omega\varepsilon} \tag{4}$$

All the previous parameters are scalars only in homogeneous

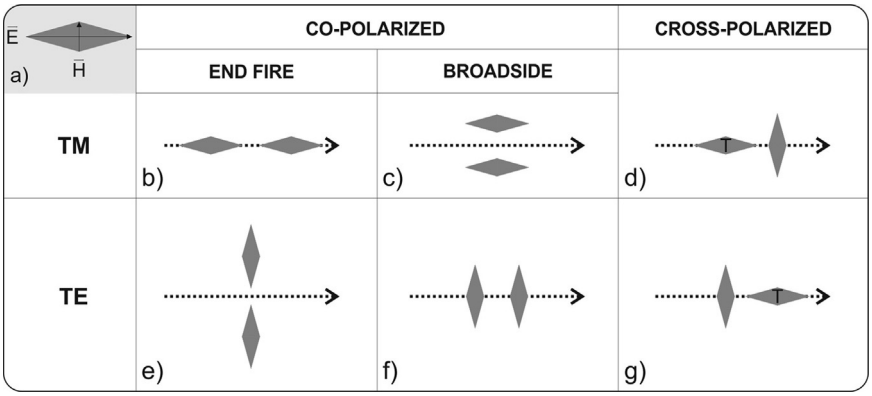

Fig. 2. Plan view of the different possible transmitter–receiver configurations. In (a) the directions of the electric (E) and magnetic (H) vectors for the considered antenna are provided. The dotted arrow indicates the survey direction.

and isotropic media, while in general they are both complex and frequency dependent. For low lossy media [30] Eq. (3) reduces to

$$v_m = c/\sqrt{\mu_r \varepsilon_r} \tag{5}$$

where ε_r is the relative dielectric permittivity (or dielectric constant) defined as the ratio between the absolute dielectric permittivity of the medium and the dielectric permittivity of free space and μ_r is the relative magnetic permeability defined as the ratio between the absolute magnetic permeability of the medium and the magnetic permeability of the free space. For non-magnetic materials, representing the most common geological media, μ_r is almost equal to 1 and can be neglected. With these assumptions the phase velocity of a plane EM wave is simply a fraction of the velocity in free space, with a constant of proportionality equal to $1/\sqrt{\varepsilon_r}$. So the velocity can be calculated with the simplified equation:

$$v_m = c/\sqrt{\varepsilon_r} \tag{6}$$

The EM wave velocity is an essential parameter of any GPR application because it is required for depth conversion from Two-Way Traveltime (TWT). Moreover, it is a crucial parameter in (a) several processing algorithms; (b) subsurface imaging; and (c) physical parameters estimation [39].

Depth conversion requires detailed knowledge of the subsurface EM velocity field, ideally at any subsurface point. The accuracy/affordability of such estimation depends on two factors: the GPR survey type and its acquisition parameters (both selected by the geophysicist) and the complexity of the subsurface. While just one or few velocity functions can be adopted in case of isotropic and moderately heterogeneous materials, and sometimes a single velocity value can approximate the actual velocity field, in most GPR applications, an accurate reconstruction of the EM velocity field is required in more complex cases. In addition, the velocity is an essential parameter in several processing algorithms (a), such as amplitude recovery, static corrections and dynamic corrections required by MF data. In particular, the amplitude corrections (both for radiation pattern and geometrical spreading) are a crucial task for any further quantitative analysis based on dynamic properties of the GPR waves and can be determined only when the EM velocities are properly estimated [39]. The EM velocity field is further essential in any imaging process (migration) aimed at reconstructing the actual subsurface structures and geometries (b). In GPR, migration is often performed by assuming a constant velocity or a very simplified velocity field. Both strategies do not take into account heterogeneity and anisotropy factors, which can be particularly important at shallow depths. So, the obtained results are only approximations of the real subsurface geometries, which may bring on mistakes and inaccuracies in the data interpretation. On the other hand, all the more sophisticated algorithms specifically implemented and proposed for GPR data imaging (e.g. [60,34,2]), as well as the ones adapted from reflection seismics [14,16,17,61,69] require a very accurate EM velocity field reconstruction in order to provide satisfactory results.

One additional use of EM velocity (c) is to provide a quantitative characterization of the materials. In fact, the subsurface EM velocity variations strongly depend not only on the rock composition, but also on fluid content and type. Therefore, from the knowledge of the EM velocity, it is possible to derive several useful petrophysical parameters such as porosity, fluid characteristics and saturation. Velocity (and other related physical parameters) are in fact increasingly used to aid the interpretation and to quantitatively characterize the subsurface in several environments (e.g. [42,86,50,79,89,73,46]).

The EM velocity field can be estimated from GPR data with different techniques that provide results with various accuracy levels. When only CO data are available, then the velocity analysis can be done by taking into account the diffracted events recorded on GPR profiles. It is in fact well known that the EM radiation generated by GPR is partly scattered when the soil contains objects having size smaller than (Rayleigh) or approximately equal to (Mie) its mean wavelength [41]. The most common velocity analysis techniques are usually reported as *Diffraction hyperbola fitting* and *Migration velocity scan*. They both exploit the shape of diffraction hyperbolas and can also be applied in an integrated way to any hyperbolic event within a GPR section. In situations where no reflections occur other methods can be applied but only in specific cases [38]. The main disadvantages are related to the attainable accuracy/resolution, since only few hyperbolas can usually be analyzed and they are irregularly distributed within the section. Moreover, in case of elongated targets like, for instance, pipes, the traveltime curve is hyperbolic only if GPR profile and target axis are almost perpendicular, otherwise it has an unpredictable shape. On the other hand, if the GPR profile is parallel to the target axis, we will not register diffractions but rather reflections from the top of the target. In real applications, the observed events are often a combination of reflections and diffractions rather than pure diffractions: in such cases, hyperbola fitting may result in incorrect estimations.

When MF data are available different velocity analysis techniques can be applied. The most common exploits the shape of the reflections on CMP gathers, which depends on the velocity of the layers above the analyzed one [88]. Considering a reflection event on a CMP gather, we can calculate the difference between the TWT (t) at a given offset and the TWT at zero offset (t_0). Such quantity

(Δt_{NMO}) is usually referred as Normal Moveout (NMO) and can be calculated from the following equation for a single horizontal reflector:

$$\Delta t_{NMO} = t - t_0 = t_0\left(\sqrt{1+\left(\frac{x}{vt_0}\right)^2} - 1\right) \tag{7}$$

In a horizontally stratified medium, the travel time equation has the form [77]

$$t = \sqrt{C_0 + C_1 x^2 + C_2 x^4 + \ldots} \tag{8}$$

in which $C_0 = t_0^2$, $C_1 = 1/v_{RMS}$, while the higher order coefficients are complicated function of travel times and velocities. The RMS velocity (v_{RMS}) down to a reflector N is defined as

$$v_{RMS} = \sqrt{\frac{1}{t_0}\sum_{i=1}^{N} v_i^2 \Delta T_i} \tag{9}$$

ΔT_i is the vertical TWT through the ith layer and $t_0 = \sum_{i=1}^{N} \Delta T_i$.

When the SSA is applicable, then Eq. (8) assumes the form:

$$t = \sqrt{t_0^2 + \frac{x^2}{v_{RMS}^2}} \tag{10}$$

that is the equation of a hyperbola. We remark that for GPR data the SSA, as well as the ones of sub-horizontal layers, are realistic only in some geological, sedimentological and glaciological cases, while are in general not satisfied for instance in archeological studies or for ultra shallow engineering applications. More complex functions can be adopted, encompassing higher order terms or other special corrections; a comprehensive review is given by Alkhalifah [1] for reflection seismic data.

The most popular techniques to estimate the velocities from CMP gathers is the semblance analysis, which is based on a coherency functional used to quantify how a recorded reflection matches different synthetic hyperbolas, each calculated for a certain velocity value. From a slightly different point of view, the RMS velocity above a given reflector can be estimated by fitting the NMO Eq. (7) with the travel-time vs. offset function [88]. The inherent NMO assumptions of planar, sub-horizontal reflectors and of smooth lateral velocity variations are often not realistic for some GPR applications. Anyway, several successful examples are reported in literature [78,42,67,68,70,9]. Semblance analysis is usually combined with manual or automated fitting of reflections by hyperbolic functions and with the Constant Velocity Gather (CVG) analysis in which the CMP is corrected for different constant velocities: the operator can then select the best velocity value for each reflected event. From the RMS velocities it is possible to compute interval velocities using Dix inversion [33] or other more complex equations that take into account also the deviations from the hyperbolic travel time [43]. Several specific studies [11,47,6,51,78,10] analyzed the possible errors affecting the velocity estimation of GPR data verifying that they are strictly site-dependent and can easily reach values of more than 10–15% [13,38,47]. Becht et al. [6] considered the influence of layer dip and of the velocity contrast, while Barrett et al. [5] and Murray et al. [63] analyzed the errors in glaciological applications.

For such reasons, other more sophisticated techniques were developed both adapting methods already proposed for reflection seismics and implementing new algorithms specifically dedicated to EM applications. One promising strategy is the pre-stack depth migration (PSDM) velocity analysis [61,66,69,70,15,16]. Such method can be iterated to reduce the estimation errors and is able to resolve spatial velocity heterogeneities on the order of one to three wavelengths at the dominant signal frequency [14]. It is based on the Common Image Gather (CIG), which is conceptually similar to a CMP but is defined only in PSDM domain. When the data are migrated with the correct EM velocity, each reflection in the CIG is imaged at a depth that is independent of offset and if the velocity model is wrong, reflectors are not flattened. This apparent offset-dependency is characterized by increasing depth with offset if the velocity above the reflector is too high or, at the opposite, decreasing depth with offset if the velocity is too low. The CIG shape can be therefore conveniently exploited for improved and well constrained velocity analyses.

Another methodology is the travel time inversion [20,48,49], but it is time and computation consuming and has limitations for complex velocity fields. A more global technique is the full waveform inversion (FWI), developed and applied to several seismic surveys with good results (e.g. [28,18]). These methods cannot be directly applied to EM waves because both amplitudes and phases of the GPR signal depend on the antenna orientation and radiation pattern [57]. In recent years new procedures have been implemented and applied on crosshole datasets [36,62]. Such methods cannot be easily adapted to ground coupled GPR system (i.e. the usual acquisition devices) because the antenna coupling depends on the subsurface material characteristics that are, in general, unknown [19]. So, approximated off-ground GPR full-waveform inversion methods have been implemented both for monostatic [56] and bistatic cases [55]. Recently, Busch et al. [19] proposed a FWI approach for surface GPR data to obtain quantitative values of the electromagnetic properties (electric conductivity, dielectric permittivity) and so to derive the subsurface velocity field. Such method has been applied only to single CMP gathers to date.

Additional specific methodologies, applicable only to MF data and in special cases, have been also implemented. Among the others, Reppert et al. [71] estimated the electric permittivity and the EM velocity by using the Brewster angle analysis on MF data, van der Kruk et al. [84] analyzed the dispersion characteristics for both TE and TM modes, while Strobbia and Cassiani [76] used guided waves for estimating soil water content of the shallow layers.

3.2. Stacking

In reflection seismics one of the basic operations applied to any MF dataset is the stacking. It sums (i.e. stacks) together all the traces of a CMP after they have been corrected for the NMO, and so after they all have zero offset. In several geophysical techniques, including GPR, there is the common practice to sum together data acquired with the same constant parameters in the same position. This process is usually called vertical stack (VS) and it is advisable to reduce random (i.e. not coherent) noises, while emphasizing the signal content. On GPR data this operation is obtained acquiring more than one trace for each profile location, recording then just the mean trace for each position. In some commercial systems VS is automatically applied, while in some other instruments the operator can fix the number of traces to be collected at each survey point. If coherent noises are present VS emphasizes both signals and such noises, leaving the signal-to-noise ratio (S/N) almost unchanged. In usual GPR acquisitions coherent noises are common and their most relevant components are related to ringing phenomena producing the so called "*Background noise*", or to undesired reflections or diffractions from objects above the surface (e.g. [64]). Other more peculiar coherent noises are for instance related to lateral waves (as shown in Fig. 6). The traces within a CMP are all related to single subsurface points, but each has a different travel path. This way, we can discriminate the reflections (having hyperbolic shape) not only from random noises, but most important from coherent ones. In other words, after the NMO corrections, each reflection will have a constant travel time

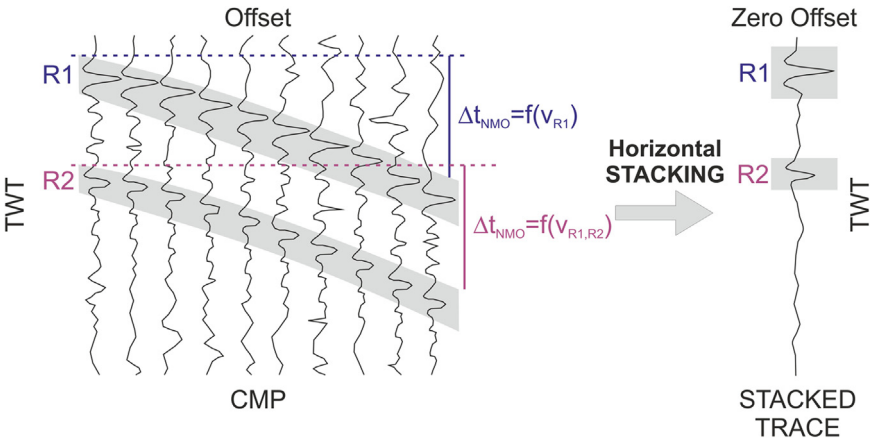

Fig. 3. Sketch of the HS for a CMP with just two reflections. After the NMO correction and the stacking the resulting trace (on the right) shows an apparent higher S/N as compared to each single CO trace of the CMP.

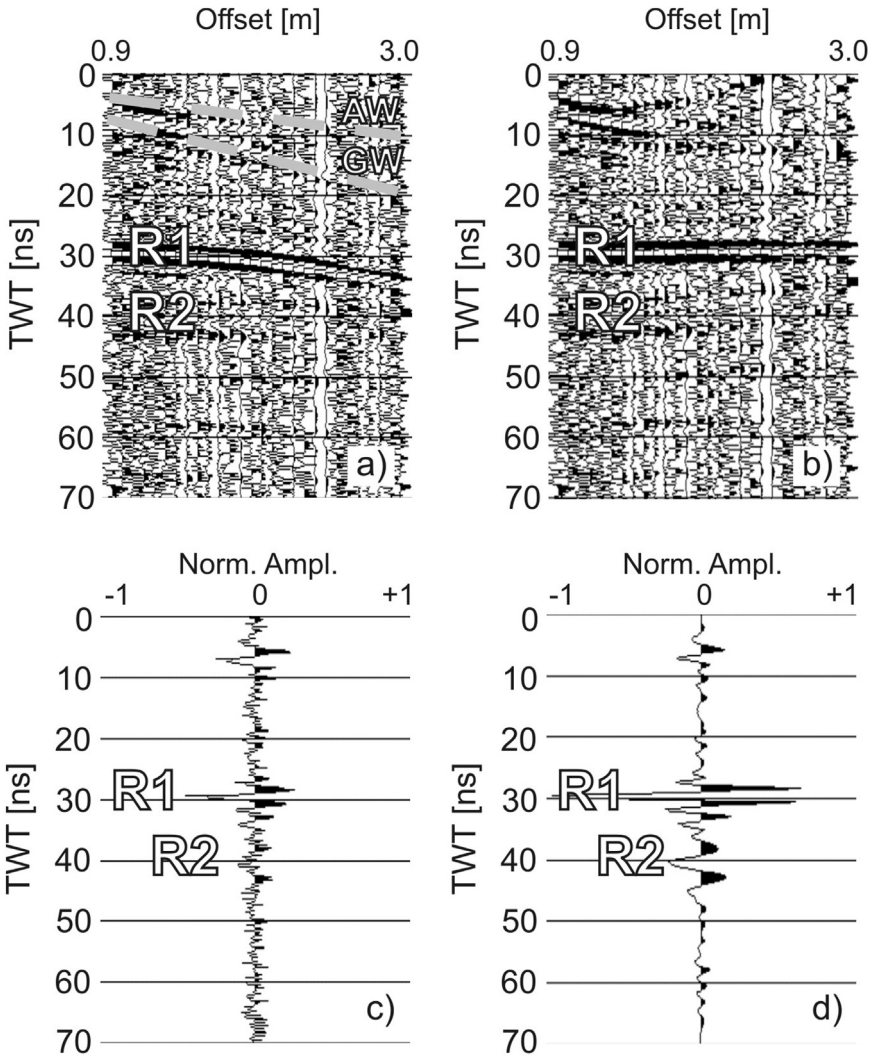

Fig. 4. Example of a real, noisy CMP of 22 traces before (a) and after (b) the NMO correction. In (c) the first trace of (b) is shown, while (d) is the trace after stacking together all the NMO corrected 22 traces: the two reflectors R1 and R2 are significantly emphasized. The two gray dashed lines in (a) mark the air wave (AW) and the ground wave (GW).

because its arrivals will be all at a virtual zero offset condition, while noises and not hyperbolic events like air and ground waves will have still an offset dependency so that after the stacking they are canceled out or, at least, significantly attenuated (Figs. 3 and 4). This second stacking type is called horizontal stack (HS), or simply stack. In order to obtain an actual S/N increment it is essential that the NMO correction is accurate for both near and far offset and that the data amplitude has been previously compensated for the different travel paths [68]. In case of dipping reflectors and in the more complex case of conflicting dips, Dip Moveout (DMO) should

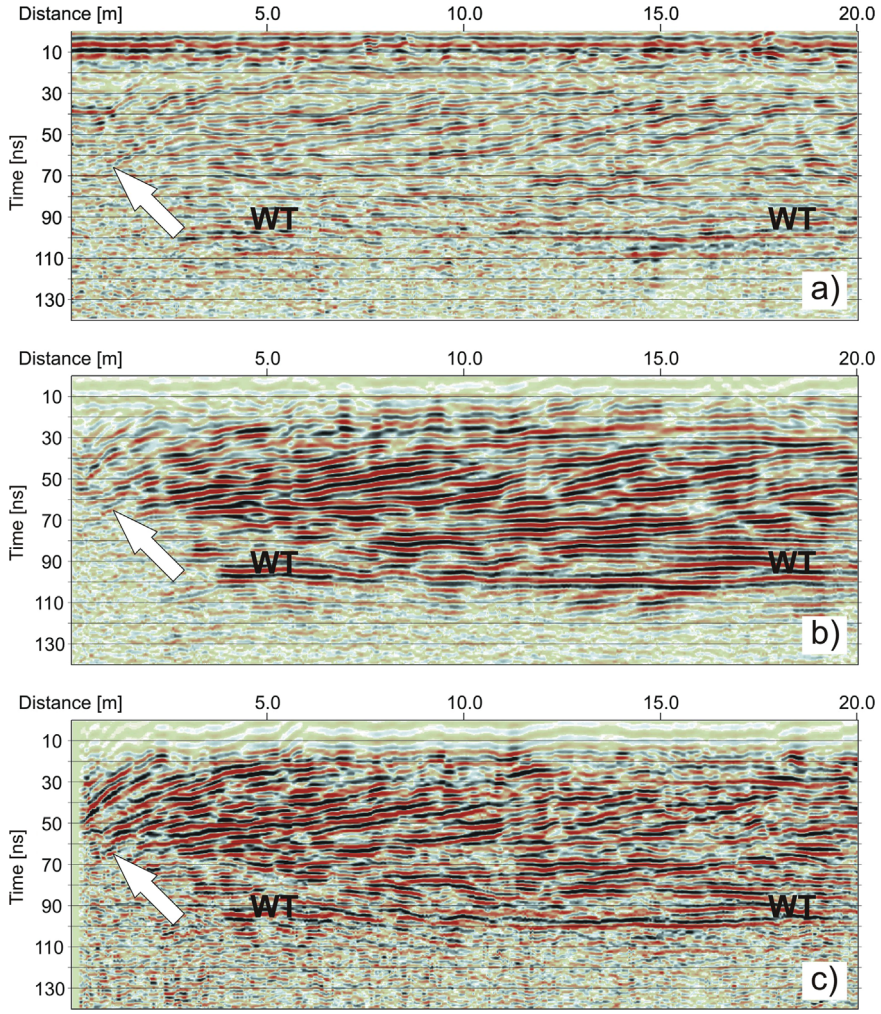

Fig. 5. Comparison between (a) a SF profile (200 MHz antennas, offset 70 cm) and (b) the corresponding stack section obtained with a maximum fold of 10 (200 MHz antennas, offsets range 70–160 cm, offset interval 10 cm). In (c) the deconvolved stack section is shown (adaptive Burg algorithm). The arrow marks a zone where strongly dipping horizons are clearer on (b) and (c) with respect to (a). WT label indicates the top of the water table.

be applied before performing accurate velocity analyses and NMO correction (see e.g. [32,70]).

The theoretic increment of S/N is equal to $\sqrt{F}$ i.e. to the root square of the fold [88]. Such result is difficult to achieve from real data since errors in the acquisition geometries, as well as the complexity of the actual EM velocity field and the subsurface structures prevent a perfect in phase stacking of the reflections. Anyway, also under such limitations HS was successfully applied in different environments allowing a substantial S/N increment [37,67,68]. An example of the whole procedure applied to a real CMP gather with a very low S/N and the comparison between a single CO trace and the stacked trace is provided in Fig. 4. The better performances of the stack trace (Fig. 4d) vs. the CO one (Fig. 4c) are apparent, especially for reflection R2, which is embedded in the noise and can be hardly recognized in the CO trace.

It is interesting to observe that a high fold is recommended (15 or 20 traces are an acceptable choice) to perform an accurate velocity analysis, while the improvements obtained from HS are significant even when CMP gathers encompass a limited trace number. Fig. 5 shows a comparison between a CO profile and the corresponding stack section obtained with a maximum fold of 10 (1000%). The interpretability of the stack section (Fig. 5b) is significantly increased especially in the deepest part, with horizons more continuous and interpretable down to at least 120 ns and so also below the water table (WT). At the opposite, on the CO section (Fig. 5a) the stratigraphic sequence is difficult to interpret especially where there are strongly dipping reflectors (marked by the white arrow) and in the central part of the section where moderately dipping horizons down to about 70 ns lie on sub-horizontal ones. Such comparison shows also a typical inherent characteristic of the stack section which has, in general, an overall lower vertical resolution compared to a CO profile. This is a consequence of the NMO correction and the HS because for real data the wavelets of the reflections are not perfectly constant at different offsets and each reflection is never perfectly horizontal. So the stacked trace has wider reflections or, in the frequency domain, wavelets shift towards lower spectral components. This is also due to an unavoidable stretching effect produced by the NMO correction that increases at large offsets, short travel times and low velocities [88]. This effect can be only partially compensated before stacking by early muting of the overly stretched segments or by filtering. The overall resolution can anyway be increased by means of post-stack deconvolution (Fig. 5c), even if unwanted high frequency noise components may be introduced by such process.

3.3. MF data analysis

MF data are not only necessary in velocity analysis and HS, but are useful in the application of dedicated techniques to

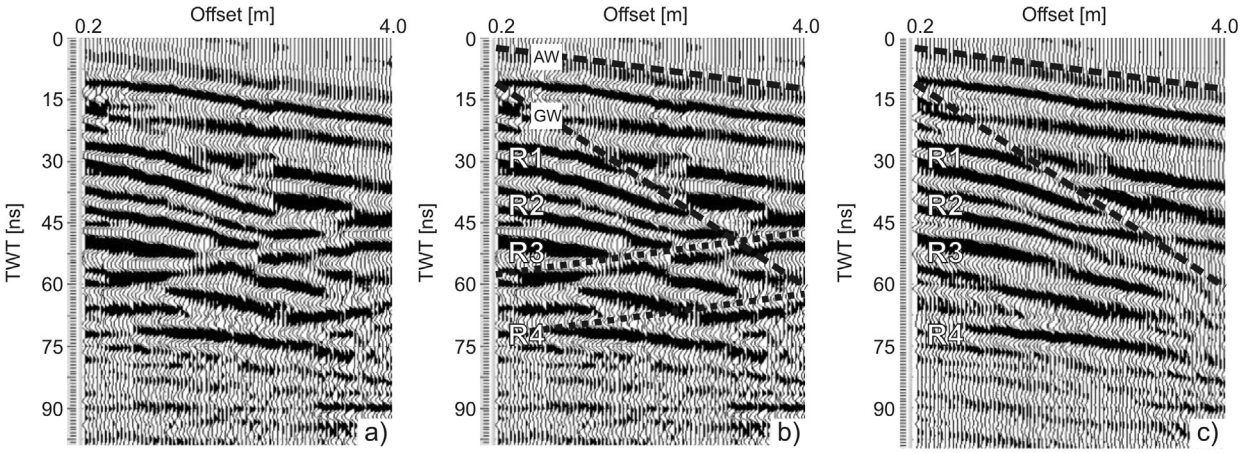

Fig. 6. Example of event recognition and selective removal on a real CMP gather: (a) processed CMP; (b) interpretation of the events (R1–R4 main reflections; AW air wave; GW ground wave; dotted line BLW); (c) the CMP after the application of a f-k filter that selectively removed the BLW leaving almost untouched the main events.

discriminate and selectively remove specific noise components. Fig. 6 provides an example. The CMP in Fig. 6a shows two parallel events characterized by decreasing TWT for increasing offset (dotted lines in Fig. 6b) besides some clear reflections (R1–R4 in Fig. 6b) and the air (AW) and the ground (GW) waves typical of any GPR dataset. The two former events are backscattered lateral waves (BLW). In this case if we analyze just one trace, which is the case of any CO acquisition, such events would be improperly interpreted as normal reflections. After their recognition, noise (and any kind of non-primary event) can be selectively removed by exploiting the peculiar moveout characteristics on CMP or other gathers. In this example the BLW were almost completely removed by a f-k filter since they opposite dip compared to any other event of the CMP. Such discussion has general validity and several analyses and processing algorithms (e.g. τ-p filters, pre-stack migrations) can be applied only if MF data are available.

3.4. Amplitude Versus Offset

When dense MF data are available, several specific data analysis procedures can be applied. Among the methods proposed we here summarize the Amplitude Versus Offset (AVO) analysis. AVO is a well established technique that is routinely applied in reflection seismic exploration to analyze the amplitudes of compressional and shear waves to detect hydrocarbons and fluid contacts (as water/oil/gas) in the reservoir (e.g. [24,25]). For EM waves the amplitude dependency is controlled by the reflection coefficients that depend on the contrast of electrical properties. Since the 1990s, several researchers analyzed the potential and the peculiarities of such technique in GPR applications to different environments. Lehmann [59] analyzed the complex reflection coefficients as a function of varying conductivity; Baker [3] discussed the applicability of AVO to contaminant detection providing both the theoretical background and some synthetic examples; Zeng et al. [90] modeled the effects of varying parameters in the Cole–Cole equation and discussed the AVO behavior. An inherent complexity of AVO response for EM waves is that it is determined by a combined effect of electric conductivity, dielectric permittivity and magnetic permeability. Numerical models indicate that the most prominent AVO effects occur when high EM contrasts are due to the presence of different rocks/sediments, but especially to variations of fluid saturation and characteristics [90]. Therefore, there are several examples of application of the AVO technique to the location and characterization of pollutants. For instance: Deeds and Bradford [31] applied AVO to detect LNAPL within an aquitard; Bradford [12] investigated a LNAPL high-conductive plume; Jordan et al. [54] exploited real data in a NAPL release; Carcione et al. [22] evaluated the AVO applicability to detect contaminants and water intrusions. Bradford and Deeds [15] analyzed in detail the effect of thin beds on AVO, estimating strengths and limitations of such technique. Such authors concluded that the AVO applicability is still limited, probably due to the difficulty of efficiently collecting continuous MF data with commercially available single-channel GPR systems, but they expect that multifold acquisition will become more efficient and more widely applied with hardware advances. On the other hand, with a specific dedicated processing, quantitative GPR AVO analyses are possible and hold significant potential as an exploratory tool, especially when combined TE and TM data are fully exploited. One still open issue is related to the processing to be applied on data before AVO analysis. In particular, a so called *true-amplitude* approach is mandatory to preserve the actual amplitude behavior. This is a critical task because the radiation pattern within the subsurface is generally unknown and so any amplitude recovery can be just a rough approximation of the actual physics of the phenomenon. In addition, there are further simplifying assumptions essential to reduce the AVO response of GPR survey to a manageable problem such as a constant antenna coupling or a negligible frequency dependency of the material properties: all such questions should be fully addressed in the future in order to extend and optimize the applicability of the method.

4. Discussion and the road ahead

In recent years a remarkable advancement in the GPR field took place thanks to the implementation of new multi-channel systems while common commercial instruments are traditionally single-channel (i.e. connected to just one transmitting and one receiving antenna). The antennas can be divided in different categories like: shielded or unshielded, air or ground coupled, as well as on the base of their polarization or typology (e.g. bow-tie, horn, resistively loaded dipoles, Vivaldi, spiral). Nowadays arrays of antennas are available for many commercial systems. An array is an obvious method of increasing the productivity rate. There are two conceptually different approaches to design arrays [53]. The first is simply to combine a number of single channel radars into a single system. The other, more interesting, is to implement the system as an integral array exploiting the increased capability related to inserting into the array antennas with different frequency, orientation, spacing. There are several examples of applications of arrays of antennas in different environments. Some workers

implemented arrays for landmine detection, which was one of the first GPR applications with very peculiar requirements and constraints [65,87]. Archeological and cultural heritage studies [40,45,58] are another typical case because it is quite common that large areas have to be investigated with high spatial resolutions. Several other applications are dedicated to engineering problems like pavement inspection or underground utility mapping [7,8].

Most of the applications of the arrays exploit just the increased productivity of the instruments, which can acquire millions of traces in a relatively short time and with high location accuracy when latest-generation GPS or total station systems are used. The virtually infinite possibility of combinations between antennas having the same or different polarizations, bandwidths, offsets, orientations, make possible to apply processing and analysis techniques that are mature from the theoretical point of view but up to now are rarely applied due to logistic constraints like, first of all, an extended acquisition time. Polarimetric analyses could be routinely implemented with dedicated acquisition geometries implemented through such multi-channel systems. Such data sets would be not only useful for AVO, but also for Amplitude Versus Azimuth (AVA) analyses exploiting the full 3-D acquisition benefits.

Rough terrains (or snake) antennas are another recent hardware implementation. Many manufacturers developed antennas dedicated to acquisitions on irregular surfaces. Such devices can have different implementations depending on the engineering details but all of them are characterized by flexible connections between the transmitter and receiver allowing, in general, a better coupling with the ground. Besides the apparent logistic advantages and the data quality improvements when applied to extremely complex conditions (forests, rocky surfaces, highly vegetated areas), further MF applications could be implemented. As far as we know, at the moment no rough terrain multi-channel system is available on the market even if its implementation is in principle feasible from the technological point of view. A flexible case (such a plastic/pvc tube) with multiple antennas inside at fixed or variable spacing, thus reproducing a kind of land streamer analog to marine seismic streamers routinely used for seismic acquisition, could further increase the feasibility and effectiveness of extensive MF GPR surveys.

5. Conclusion

MF GPR allows to obtain enhanced subsurface images and quantitative information about physical properties of the materials if compared with the usual CO techniques. The EM velocity field represents the most important information that can be extracted from field data and, except some peculiar cases, it can be estimated with sufficient accuracy and confidence only when MF data are available. From the velocity field several other properties can be derived or correlated thanks to the existing theoretical physical laws as well as empirical or semi-empirical equations. Porosity, water or other fluids content, dielectric permittivity, bulk electric conductivity, density of frozen materials, fluid saturation, moisture content, intrinsic EM attenuation, hydraulic conductivity, are some of the physical parameters which can be assessed. The inherent limitations of the velocity estimation performed on CO data reduce the accuracy of any derived quantity, while MF acquisitions can partially overcome such problem.

HS is a conceptually simple and effective way to recognize and suppress both random and coherent noise. An improved S/N allows to reach larger investigation depths in many real cases. This is a crucial point when using a geophysical system like GPR, which has intrinsic depth limitations especially when used in moderate to high electrical conductive environments. Most of the methodologies summarized in this paper are adapted from reflection seismic and are robust, mature and tested even in challenging conditions. We are confident that the GPR technique could further advance by just exploiting the full range of processing and inversion options that is offered by contiguous wave-equation based geophysical methods (such as e.g. 3-D multi-component seismic). Recent theoretical advancements in imaging, full waveform inversion, as well as specific attribute analysis exploiting the peculiar frequency dependency and attenuation of EM waves could provide additional elements for methodological improvement. At the same time, the increasing diffusion of array of antennas or other innovative solutions in the antenna design and manufacturing, could sensibly reduce the field work, while increasing the amount of recorded information, so widening the applicability of the GPR technique and improving the quality of the results.

Acknowledgments

This research is partially supported by the “Finanziamento di Ateneo per progetti di ricerca scientifica – FRA 2014” of the University of Trieste. We gratefully acknowledge Halliburton through the University of Trieste Landmark academic grant. We are grateful to Luca Baradello for our past fruitful discussions about Multi-fold GPR data. We also thank the guest editor Nikos Economou for his kind invitation to write this review paper, and two anonymous reviewers for their suggestions.

References

[1] T. Alkhalifah, Velocity analysis using nonhyperbolic moveout in transversely isotropic media, Geophysics 62 (1997) 1839–1854.
[2] N. Allroggen, J. Tronicke, M. Delock, U. Böniger, Topographic migration of 2D and 3D ground-penetrating radar data considering variable velocities, Near Surf. Geophys. 13 (3) (2015) 253–259.
[3] G.S. Baker, Applying AVO analysis to GPR data, Geophys. Res. Lett. 25 (1998) 397–400.
[4] C.A. Balanis, Advanced Engineering Electromagnetics, Wiley 1989, p. 981.
[5] B.E. Barrett, T. Murray, R. Clark, Errors in radar CMP velocity estimates due to survey geometry, and their implication for ice water content estimation, J. Environ. Eng. Geophys. 12 (1) (2007) 101–111.
[6] A. Becht, E. Appel, P. Dietrich, Analysis of multi-offset GPR data: a case study in a coarse grained gravel aquifer, Surf. Geophys. 4 (2006) 227–240.
[7] A. Benedetto, A three dimensional approach for tracking cracks in bridges using GPR, J. Appl. Geophys. 97 (2013) 37–44.
[8] R. Birken, D.E. Miller, M. Burns, P. Albats, R. Casadonte, R. Deming, T. Derubeis, T. Hansen, M. Oristaglio, Efficient large-scale underground utility mapping in New York City using a multi-channel ground-penetrating imaging radar system, in: Proceedings of the GPR 2002, 9th International Conference on Ground Penetrating Radar, Expanded Abstracts, 2002, pp. 186-191.
[9] A.D. Booth, N.T. Linford, R.A. Clark, T. Murray, Three-dimensional, multi-offset GPR imaging of archaeological targets, Archaeol. Prospect. 15 (2008) 1–20.
[10] A.D. Booth, R. Clark, T. Murray, Semblance response to a ground-penetrating radar wavelet and resulting errors in velocity analysis, Surf. Geophys. 8 (3) (2010) 235–246.
[11] A.D. Booth, R. Clark, T. Murray, Influences on the resolution of GPR velocity analyses and a Monte Carlo simulation for establishing velocity precision, Surf. Geophys. 9 (5) (2011) 399–411.
[12] J.H. Bradford, GPR offset dependent reflectivity analysis for characterization of a high-conductivity LNAPL plume, in: Proceedings of Symposium on the application of geophysics to engineering and environmental problems (SAGEEP), San Antonio, TX, 2003, pp. 238–252.
[13] J.H. Bradford, J.T. Harper, Wave field migration as a tool for estimating spatially continuous radar velocity and water content in glaciers, Geophys. Res. Lett. 32 (L08502) (2005) 1–4.
[14] J.H. Bradford, Applying reflection tomography in the postmigration domain to multifold ground-penetrating radar data, Geophysics 71 (1) (2006) K1–K8.
[15] J.H. Bradford, J.C. Deeds, Ground-penetrating radar theory and application of thin-bed offset-dependent reflectivity, Geophysics 71 (3) (2006) K47–K57.
[16] J.H. Bradford, J. Nichols, D. Mikesell, J. Harper, Continuous multi-fold acquisition and analysis of ground-penetrating radar data for improved characterization of glacier structure and water content, Ann. Glaciol. 50 (2009) 1–9.
[17] J.H. Bradford, J. Nichols, D. Mikesell, J.T. Harper, Continuous profiles of electromagnetic wave velocity and water content in glaciers: an example from

Bench Glacier, Alaska, USA, Ann. Glaciol. 50 (51) (2009) 1–9.
[18] R. Brossier, S. Operto, J. Virieux, Seismic imaging of complex onshore structures by 2D elastic frequency-domain full-waveform inversion, Geophysics 74 (6) (2009) WCC105–WCC118.
[19] S. Busch, J. van der Kruk, J. Bikowski, H. Vereecken, Quantitative conductivity and permittivity estimation using full-waveform inversion of on-ground GPR data, Geophysics 77 (6) (2012) H79–H91.
[20] J. Cai, G.A. McMechan, 2-D ray-based tomography for velocity, layer shape, and attenuation from GPR data, Geophysics 64 (5) (1999) 1579–1593.
[21] J.M. Carcione, F. Cavallini, On the acoustic-electromagnetic analogy, Wave Motion 21 (1995) 149–162.
[22] J.M. Carcione, D. Gei, M.A.B. Botelho, A. Osella, M. de la Vega, Fresnel reflection coefficients for GPR-AVO analysis and detection of seawater and NAPL contaminants, Surf. Geophys. 4 (2006) 253–263.
[23] J.M. Carcione, Wave Propagation in Anisotropic, Anelastic, Porous and Electromagnetic Media, 2nd ed., Elsevier Science & Technology Wave fields in real media 2007, p. 538.
[24] J.P. Castagna, AVO analysis – tutorial and review, in: J.P. Castagna, M.M. Backus (Eds.), Offset-dependent Reflectivity – Theory and Practice of AVO Analysis: Investigation in Geophysics, SEG, 1993, pp. 3–36.
[25] J.P. Castagna, M.L. Batzle, T.K. Kan, Rock physics – the link between rock properties and AVO response, in: J.P. Castagna, M.M. Backus (Eds.), Offset-dependent Reflectivity – Theory and practice of AVO analysis: Investigation in Geophysics, SEG, 1993, pp. 135–171.
[26] S. Chopra, K.J. Marfurt, Seismic Attributes for Prospect Identification and Reservoir Characterization, SEG/EAGE, 2007 464 pp.
[27] L.B. Conyers, Ground-penetrating Radar for Archaeology, Alta Mira Press, Walnut Creek, CA, 2004.
[28] E. Crase, A. Pica, M. Noble, J. McDonald, A. Tarantola, Robust elastic nonlinear wave-form inversion – application to real data, Geophysics 55 (5) (1990) 527–538.
[29] D.J. Daniels, Ground Penetrating Radar, 2nd edition, Radar, Sonar, Navigation and Avionics Series, vol. 15, Institute of Electrical Engineers, London, UK, 2004.
[30] J.L. Davis, A.P. Annan, Ground-penetrating radar for high-resolution mapping of soil and rock stratigraphy, Geophys. Prospect. 37 (5) (1989) 531–551.
[31] J.C. Deeds, J.H. Bradford, Characterization of an aquitard and direct detection of LNAPL at Hill Air Force Base using GPR AVO and migration velocity analysis, in: Proceedings of the 9th International Conference on Ground Penetrating Radar, International Society for Optical Engineering, Proceedings, 2002, pp. 323–329.
[32] S.M. Deregowsky, F. Rocca, Geometrical optics and wave theory for constant-offset sections in layered media, Geophys. Prospect. 29 (1981) 374–406.
[33] C.H. Dix, Seismic velocity from surface measurements, Geophysics 34 (1955) 180–195.
[34] J.-R. Dujardin, M. Bano, Topographic migration of GPR data: examples from Chad and Mongolia, Cold Reg. Geosci. 345 (2013) 73–80.
[35] E.G. Ernenwein, Imaging in the Ground-penetrating radar near-field zone: a case study from New Mexico, USA, Archaeol. Prospect. 13 (2006) 155–158.
[36] J.R. Ernst, A.G. Gree, H. Maurer, K. Holliger, Application of a new 2D time-domain full-waveform inversion scheme to crosshole radar data, Geophysics 72 (5) (2007) J53–J64.
[37] E. Fisher, M. George, P. Annan, Acquisition and processing of wide-aperture ground-penetrating radar data, Geophysics 57 (1992) 495–504.
[38] E. Forte, M. Dossi, R.R. Colucci, M. Pipan, A new fast methodology to estimate the density of frozen materials by means of common offset GPR data, J. Appl. Geophys. 99 (2013) 135–145.
[39] E. Forte, M. Dossi, M. Pipan, R.R. Colucci, Velocity analysis from Common Offset GPR data inversion: theory and application to synthetic and real data, Geophys. J. Int. 197 (3) (2014) 1471–1483.
[40] R.G. Francese, E. Finzi, G. Morelli, 3-D high-resolution multi-channel radar investigation of a Roman village in Northern Italy, J. Appl. Geophys. 67 (2009) 44–51.
[41] M. Grasmueck, R. Weger, H. Horstmeyer, Full-resolution 3D GPR imaging, Geophysics 70 (1) (2005) K12–K19.
[42] R. Greaves, D. Lesmes, J. Lee, M. Toksoz, Velocity variations and water content estimated from multi-offset, ground-penetrating radar, Geophysics 61 (1996) 683–695.
[43] V. Gretchka, I. Tsvankin, J.K. Cohen, Generalised Dix equation and modeling of normal moveout in inhomogeneous media, in: Proceedings of the 67th Annual International Meeting, SEG 1997, 1997.
[44] P. Gudmandsen, Electromagnetic probing of ice, in: J.R. Wait (Ed.), Electromagnetic Probing in Geophysics, The Golem Press, CO, 1971, pp. 321–348.
[45] J. Gustafsson, M. Alkarp, Array GPR investigation of the cathedral of Uppsal, Surf. Geophys. 5 (2007) 203–207.
[46] G. Hamann, J. Tronicke, C. Steelman, A. Endres, Spectral velocity analysis for determination of ground wave velocities and their uncertainties in multi-offset GPR data, Surf. Geophys. 11 (2013) 167–176.
[47] G. Hamann, J. Tronicke, Global inversion of GPR traveltimes to assess uncertainties in CMP velocity models, Surf. Geophys. 12 (2014) 505–514.
[48] S. Hanafy, S.A. Hagrey, Ground-penetrating radar tomography for soil-moisture heterogeneity, Geophysics 71 (1) (2006) k9–k18.
[49] J.T. Harper, J.H. Bradford, Snow stratigraphy over a uniform depositional surface: spatial variability and measurement tools, Cold Reg. Sci. Technol. 37 (3) (2003) 289–298.
[50] J.A. Huisman, S.S. Hubbard, J.D. Redman, A.P. Annan, Measuring soil water content with ground penetrating radar: a review, Vadose Zone J. 2 (2003) 476–491.
[51] R.W. Jacob, J.F. Hermance, Assessing the precision of GPR velocity and vertical two-way travel time estimates, J. Environ. Eng. Geophys. 9 (2004) 143–153.
[52] M. Jeannin, S. Garambois, C. Grégoire, D. Jongmans, Multiconfiguration GPR measurements for geometric fracture characterization in limestone cliffs (Alps), Geophysics 71 (3) (2006) B85–B92.
[53] H.M. Jol, Ground Penetrating Radar: Theory and Applications, Elsevier 2009, p. 534.
[54] T.E. Jordan, S.B. Baker, K. Henn, J.-P. Messier, Using amplitude variations with offset and normalized residual polarization analysis of ground penetrating radar data to differentiate a NAPL release from stratigraphic changes, J. Appl. Geophys. 56 (1) (2004) 41–58.
[55] A. Kalogeropoulos, J. van der Kruk, J. Hugenschmidt, S. Busch, K. Merz, Chlorides and moisture assessment in concrete by GPR full waveform inversion, Surf. Geophys. 9 (2011) 277–285.
[56] S. Lambot, E.C. Slob, I. van den Bosch, B. Stockbroeckx, B. Scheers, M. Vanclooster, Estimating soil electric properties from monostatic ground-penetrating radar signal inversion in the frequency domain, Water Resour. Res. 40 (W04205) (2004) 1–12.
[57] B. Lampe, K. Holliger, Effects of fractal fluctuations in topographic relief, permittivity and conductivity on ground-penetrating radar antenna radiation, Geophysics 68 (6) (2003) 1934–1944.
[58] J. Leckebusch, Use of antenna arrays for GPR surveying in archaeology, Surf. Geophys. 3 (2005) 109–113.
[59] F. Lehmann, Fresnel equations for reflection and transmission at boundaries between conductive media, with applications to georadar problems, in: Proceedings of the 6th International Conference on Ground-Penetrating Radar, International Society for Optical Engineering, 1996, pp. 555–560.
[60] F. Lehmann, A.G. Green, Topographic migration of georadar data: Implications for acquisition and processing, Geophysics 65 (3) (2000) 836–848.
[61] D. Leparoux, D. Gibert, P. Cote, Adaptation of prestack migration to multi-offset ground-penetrating radar (GPR) data, Geophys. Prospect. 49 (2001) 374–386.
[62] G.A. Meles, J. Van der Kruk, S.A. Greenhalgh, J.R. Ernst, H. Maurer, A.G. Green, A new vector waveform inversion algorithm for simultaneous updating of conductivity and permittivity parameters from combination of crosshole/borehole-to-surface GPR data, IEEE Trans. Geosci. Remote Sens. 48 (2010) 3391–3407.
[63] T. Murray, A. Booth, D.M. Rippin, Water-content of glacier-ice: limitations on estimates from velocity analysis of surface ground-penetrating radar surveys, J. Environ. Eng. Geophys. 12 (1) (2007) 87–99.
[64] L. Nuzzo, Coherent noise attenuation in GPR data by linear and parabolic Radon Transform techniques, Ann. Geophys. 46 (3) (2003) 533–547.
[65] L. Nuzzo, G. Alli, R. Guidi, N. Cortesi, A. Sarri, G. Manacorda, A new densely-sampled Ground Penetrating Radar array for landmine detection, in: Proceedings of the 15th International Conference on Ground Penetrating Radar, June 30–July 4, 2014, Brussels, Belgium.
[66] H. Perroud, M. Tygel, Velocity estimation by the common-reflection-surface (CRS) method: Using ground-penetrating radar data, Geophysics 70 (6) (2005) B43–B52.
[67] M. Pipan, I. Finetti, F. Ferigo, Multi-fold GPR techniques with applications to High-Resolution studies: two case histories, Eur. J. Environ. Eng. Geophys. 1 (1) (1996) 83–103.
[68] M. Pipan, L. Baradello, I. Finetti, E. Forte, A. Prizzon, 2-D and 3-D processing and interpretation of multi-fold ground penetrating radar data: a case history from an archaeological site, J. Appl. Geophys. 41 (2–3) (1999) 271–292.
[69] M. Pipan, E. Forte, G. Dal Moro, M. Sugan, I. Finetti, Multifold ground-penetrating radar and resistivity to study the stratigraphy of shallow unconsolidated sediments, Lead. Edge 22 (9) (2003) 876–881.
[70] M. Pipan, E. Forte, G. Dal Moro, M. Sugan, I. Finetti, Multi-fold, multi-component and multi-azimuth GPR for subsurface imaging and material characterization, in: D. Daniels (Ed.), Ground Penetrating Radar, 2nd Edition, IEE Books, UK, 2004.
[71] P.M. Reppert, F.D. Morgan, M.N. Toksöz, Dielectric constant determination using ground penetrating radar reflection coefficients, J. Appl. Geophys. 43 (2000) 189–197.
[72] R.E. Sheriff, L.P. Geldart, Exploration Seismology, Cambridge University Press, 1995.
[73] C.M. Steelman, A.L. Endres, Assessing vertical soil moisture dynamics using multi-frequency GPR common-midpoint soundings, J. Hydrol. 51 (66) (2012) 436–437.
[74] R. Streich, J. van der Kruk, Characterizing a GPR antenna system by near-field measurements, Geophysics 72 (5) (2007) A51–A55.
[75] R. Streich, J. van der Kruk, Accurate imaging of multicomponent GPR data based on exact radiation patterns, IEEE Trans. Geosci. Remote Sens. 45 (2007) 93–103.
[76] C. Strobbia, G. Cassiani, Multilayer ground-penetrating radar guided waves in shallow soil layers for estimating soil water content, Geophysics 72 (4) (2007) J17–J29.
[77] M.T. Taner, F. Koehler, Velocity spectra – digital computer derivation and applications of velocity functions, Geophysics 34 (1969) 859–881.
[78] S. Tillard, J.C. Dubois, Analysis of GPR data: wave propagation velocity determination, J. Appl. Geophys. 33 (1995) 77–91.
[79] J. Tronicke, K. Holliger, W. Barrash, M.D. Knoll, Multivariate analysis of cross-hole georadar velocity and attenuation tomograms for aquifer zonation, Water Resour. Res. 40 (W01519) (2004) 1–14.
[80] B. Ursin, Review of elastic and electromagnetic wave propagation in

horizontally layered media, Geophysics 48 (1) (1983) 1063–1081.
[81] S. Valle, L. Zanzi, M. Sgheiz, G. Lenzi, J. Friborg, Ground Penetrating Radar Antennas: Theoretical and experimental directivity functions, IEEE Trans. Geosci. Remote Sens. 39 (4) (2001) 749–758.
[82] J. Van der Kruk, C.P.A. Wapenaar, J.T. Fokkema, P.M. van der Berg, Improved three-dimensional image reconstruction technique for multi-component ground penetrating radar data, Subsurf. Sens. Technol. Appl. 4 (2003) 61–99.
[83] J. Van der Kruk, C.P.A. Wapenaar, J.T. Fokkema, P.M. van der Berg, Three-dimensional imaging of multicomponent ground-penetrating radar data, Geophysics 68 (4) (2003) 1241–1254.
[84] J. van der Kruk, R. Streich, A.G. Green, Properties of surface waveguides derived from separate and joint inversion of dispersive TE and TM GPR data, Geophysics 71 (1) (2006) K19–K29.
[85] J.P. van Gestel, P.L. Stoffa, Application of Alford rotation to ground-penetrating radar data, Geophysics 66 (6) (2001) 1781–1792.
[86] R.A. van Overmeeren, S.V. Sariowan, J.C. Gehrels, Ground penetrating radar for determining volumetric soil water content; results of comparative measurements at two test sites, J. Hydrol. 197 (1997) 316–338.
[87] A.G. Yarovoy, T.G. Savelyev, P.J. Aubry, P.E. Lys, L.P. Ligthart, UWB array-based sensor for near-field imaging, IEEE Trans. Microw. Theory Tech. 55 (2007) 1288–1295.
[88] Yilmaz, Ö., Seismic Data Analysis: Processing, Inversion and Interpretation of Seismic Data, 2nd ed., SEG, 2001, 998 pp.
[89] U. Wollschläger, H. Gerhards, Q. Yu, K. Roth, Multi-channel ground-penetrating radar to explore spatial variations in thaw depth and moisture content in the active layer of a permafrost site, Cryosphere 4 (2010) 269–283.
[90] X. Zeng, G.A. McMechan, T. Xu, Synthesis of amplitude-versus-offset variations in ground-penetrating radar data, Geophysics 65 (1) (2000) 113–125.